J. Materials, Conc. Struct. Pavements, JSCE, No. 690/V-53, 147-158, 2001 November

ANALYSIS OF RC PANELS AND POST-PEAK BEHAVIOR USING UNIFIED PLASTIC MODEL

Mohammad Reza SALAMY[1] and Tada-aki TANABE[2]

[1]Member of JSCE, Dr. of Eng., Oriental Construction Co. (Nagoya Mitsui South Build., 4-27-20,Mei-eki, Nakamura-ku, Nagoya 450-0002, Japan)
[2]Fellow of JSCE, Dr. of Eng., Professor, Dept. of Civil Eng., Nagoya University (Furo cho 1, Chikusa ku, Nagoya 464-8603, Japan)

In this paper, a unified plastic model for concrete, in which only one criterion is considered to describe the behavior of concrete under different stress states, is used. This model can treat a major nonlinear phenomenon of concrete such as cracking; shear transfer degradation, tension stiffening and compressive strength reduction. The objective of this paper is to follow mentioned method together with presented formulation based on complementary matrix to analyze localized failure of RC panels as well as post-peak behavior while shear band is formed. This phenomenon occurs when the material acoustic tensor **A(n)** looses its positive definiteness and usually takes place when RC element fails in shear.

Key Words : *reinforced concrete, localization, complementary matrix, shear band, non-associated flow rule*

1. INTRODUCTION

Post-peak analysis of structures has become an important research topic in recent years particularly for those analyses of structures under seismic loads. In this regard, a large number of research work have been conducted to predict post-peak behavior of RC structures but the experimental observations are not yet enough to provide strong evidence for presented methods. The most recent works in post-peak analysis is given in reference 15. In this paper, most consideration is to predict post-peak behavior of RC structures and develop a method in localization analysis framework and shear band formation. For this purpose, any proper constitutive model to obtain material stiffness tensor can be used in the presented method.

Most of the already presented methods by other researchers are for using in finite element formulation while just a few works have been done in constitutive equation level for localization study[1),2)]. Application of localization by means of finite element with embedded localization zone presented by Belytschko *et al.*[3)] has been tried for RC shear walls as well as RC beams in previous works[4),5)]. This study is dedicated to the modeling of the shear band localization in context of constitutive equation level of material based on modified Drucker-Prager[6)] yield function. The basic constitutive model, which is used in localization analysis here to define post-peak regime was originally presented by Tanabe *et al.*[6)] as a unified constitutive model for reinforced concrete elements.

Yu, G.[14)] used this model in his localization analysis in constitutive equation level without considering localized zone bandwidth after localization. In his works, analysis in constitutive equation level is independent to shear bandwidth and in fact, all parts of the structure are loading after localization without any unloading region. Accordingly, strain jump, which is a result of different strain of two loading and unloading parts, will never take place. In the presented study, similar constitutive model is used for pre-peak regime while after localization, constitutive equation is modified in section 3 by means of complementary matrix and shear bandwidth is taken into account. Based on shear bandwidth as well as material properties of localized part, post-peak regime can be predicted via presented formulation.

Two criterions are selected to define peak point as well as shear band formation within an element. The first criterion is related to determinant of acoustic tensor. Once acoustic tensor looses its positive definiteness, it signals localization and shear band formation. It is found that the exact point of shear band formation and peak point of loading are not always coincided to each other specially for non-associated plasticity analysis, hence Druker's

stability postulate is used as second criterion to define the exact point of the peak.

Since the calculation here is based on strain field, using complementary matrix to go beyond peak point of loading is found an efficient method rather than stiffness matrix. The authors tried stiffness matrix as well but it was very complicated to reach an explicit formulation to use in computational analysis of post-peak regime. This complication manifests itself in parametric study much seriously. The method is also applied to predict a special form of instability so-called snap-back. This kind of behavior might occur in some kind of shear failure in which shear band has been formed and bandwidth is comparatively thin. Numerically, this kind of instability can be captured by the Arc-length method[7), 8)] but not in constitutive equation level of calculation.

Analytically, shear band is formed due to accumulation of strain inside this band while in the neighboring points, strain reduces as a result of elastic unloading so strain field shows a jump and discontinuity in the border of shear band. This phenomenon is usually called localization. According to Hill[9)], a shear band is considered as a thin material layer that is bounded by two material discontinuity surfaces of the velocity gradient. A major motivation to determine analytically the critical bifurcation directions is the interest in localization phenomenon that has been displayed in recent years in the context of finite element analysis. To capture localized deformation patterns along the characteristics, the element mesh may be designed accordingly or enriched with the special shape function as described by Ortiz *et al.*[10)]. This model has been used by Salamy *et al.*[5)] in FEM context but in this study, discontinuity plane is considered and formulated in constitutive equation level analysis.

This localization condition describes the formation of a discontinuity in the field of velocity gradients across a surface defined by the normal vector **n**. Discontinuous bifurcation is signaled by a singularity of the acoustic or localization tensor **A(n)** when $det\mathbf{A}(\mathbf{n})=0$. Solving the mentioned equation for vector **n** gives direction of shear band.

The results of well-known experiments done by Vecchio and Collins[11)] are used for evaluation of the method in pre-peak prediction of RC elements failed in either *Mode-I* or *Mode-II*. Unfortunately, the homogeneous stress states desirable in material testing lead to instability near peak; for this reason, much of the available data restricted to the pre-peak regime, resulting in a scarcity of test data for calibration and verification of post-peak material formulation. A very stiff or servo-controlled test apparatus is necessary to mimic the constrained condition of actual concrete structures. The authors could not find any experimental results to calibrate accuracy of the method for post-peak regime but believe that the results are reasonable although evaluation of the results by reliable experimental observation is necessary.

2. CONSTITUTIVE EQUATION FOR REINFORSED CONCRETE ELEMENT

Reinforced concrete elements can be treated as a composite material and both reinforcement and concrete have been modeled as elasto-plastic types of materials. For concrete as a softening material, modified Drucker-Prager yield criterion[6)] is presented in this section and as can be seen later, tension stiffening effect, influences of reinforcement ratio as well as compression deterioration of concrete have been considered in this model. As a composite material, reinforced concrete constitutive matrix $\mathbf{D}_{RC}$ can be obtain by

$$\mathbf{D}_{RC} = \mathbf{D}_S + \mathbf{D}_C \tag{1}$$

where $\mathbf{D}_S$ and $\mathbf{D}_C$ are tangential constitutive matrix of steel and concrete respectively.

(1) Constitutive model of reinforcement

The constitutive model of the reinforcement is assumed to be given by an elasto-plastic model with a linear elastic stiffness by

$$\mathbf{D}_S = \begin{bmatrix} \rho_x E_x & 0 & 0 \\ 0 & \rho_y E_y & 0 \\ 0 & 0 & 0 \end{bmatrix} \tag{2}$$

in which ρ_x and ρ_y are the reinforcement ratios and E_x and E_y are the Young's modulus of the reinforcement in the X and Y directions respectively. The shear stiffness of the reinforcement is assumed to be equal to zero.

If the reinforcements are in local directions (x,y) which is not coincide to global direction of concrete (X,Y) hence steel stiffness matrix is transferred to global coordinate system as follow

$$\mathbf{D}_S = \mathbf{T}_\theta^T \, \mathbf{D}_S \, \mathbf{T}_\theta \tag{3}$$

where θ is angle of reinforcement direction or angle between local coordinates (x,y) and global coordinates (X,Y). In Eq.(3), the transformation matrix of steel stiffness $\mathbf{T}_\theta$ is

$$T_\theta = \begin{bmatrix} C^2 & S^2 & CS \\ S^2 & C^2 & -CS \\ -2CS & 2CS & C^2-S^2 \end{bmatrix}, \quad \begin{matrix} C=\cos\theta \\ S=\sin\theta \end{matrix} \qquad (4)$$

After reaching the uniaxial tensile strength of f_{yt} or uniaxial compressive strength of f_{yc} in the reinforcement, related items in the stiffness matrix set by zero. In other words, hardening of steel after yielding is neglected in this model and perfect plastic behavior is assumed.

(2) Modified Drucker-Prager failure surface for concrete

The Drucker-Prager yield function is widely used in plasticity based analysis of pressure sensitive material such as concrete and rock. This criterion gives acceptable results for plain concrete while needs to be modified for concrete cooperated with reinforcement. It has been recognized that the major nonlinear factors for concrete in reinforced concrete structures can be briefly categorized in three items as follows:

1. Tension stiffening effect
2. Compression strength reduction due to transverse tensile strain
3. Shear transfer at the crack surface

Aforementioned items should be considered in a comprehensive model. The already existing models can perhaps correctly reflect one of these various kinds of non-linearity effects but fail to deal with others. Therefore we may encounter the judgment problem of appropriateness of choice of various nonlinear models for above factors. For these reasons, it is worthwhile using a unified plastic concrete model[6] in which only one criterion is used to describe the various nonlinear behavior of concrete under different stress states including tension stiffening and compressive strength reduction. Modified Drucker-Prager failure surface (**Fig.1**), which is used in this paper, can be expressed as follow:

$$f = J_2 - (k_f - \alpha_f I_1)^2 + (k_f - \alpha_f \eta)^2 \qquad (5)$$

Moreover, a similar expression for the plastic potential function is assumed as

$$g = J_2 - (k_g - \alpha_g I_1)^2 + (k_g - \alpha_g \eta)^2 \qquad (6)$$

where $I_1 = \sigma_{kk}$ and $J_2 = \frac{1}{2} s_{ij} s_{ij}$ are the first invariant of stress tensor σ_{ij} and the second invariant of deviatoric tensor s_{ij} respectively. Parameters α_f, k_f, α_g and k_g are material constants. According to the cohesion c, the internal friction angle ϕ, α_f and k_f are defined as

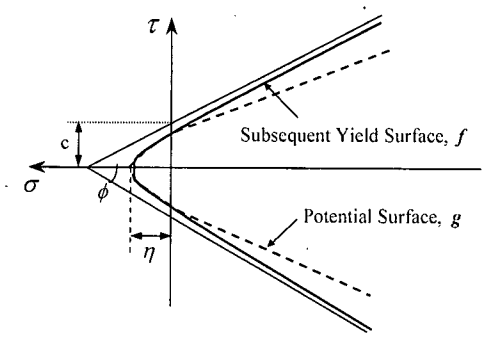

Fig.1 Yielding and Potential Surfaces

$$k_f = \frac{6c\cos\phi}{\sqrt{3}(3+y\sin\phi_1)} \qquad (7)$$

$$\alpha_f = \frac{2\sin\phi}{\sqrt{3}(3+y\sin\phi_1)} \qquad (8)$$

where ϕ_1 is constant ($\phi_1 = 14^0$) and the function of y is defined as

$$y = \sqrt{a(\cos 3\theta + 1) + 0.01} - 1.10 \qquad (9)$$

where $a = \frac{1}{2} r^2 + 2.1r + 2.2$ and

$$r = \begin{cases} 3.14 & I_1 \le f_c' \\ 2.93\cos(\frac{I_1}{f_c'}\pi) + 6.07 & f_c' < I_1 \le f_t \\ 9.0 & I_1 > f_t \end{cases} \qquad (10)$$

where $\cos 3\theta = 3\sqrt{3} J_3 / 2 J_2^{\frac{3}{2}}$ and $J_3 = \frac{1}{3} s_{ij} s_{jk} s_{ki}$ is the third invariant of the deviatoric tensor s_{ij}. The notation ϕ and c are two strength parameters in Mohr-Coulomb criterion namely so-called mobilized friction angle and mobilized cohesion which are not constant but depend on the plastic strain history through the damage parameter ω. Possible relations for hardening and softening model are suggested as follows.

$$c = c_0 \exp[-(m\omega)^2] \qquad (11)$$

$$\phi = \begin{cases} \phi_0 + (\phi_f - \phi_0)\sqrt{2\omega - \omega^2} & \omega \le 1 \\ \phi_f & \omega > 1 \end{cases} \quad (12)$$

where m is material constant.

The notation c_0, ϕ_0 and ϕ_f denote the initial cohesion, the initial internal friction angle and the final internal friction angle of concrete respectively. In the similar manner, k_g and α_g are defined as

$$k_g = \frac{6c\cos\psi}{\sqrt{3}(3 + y\sin\phi_1)} \quad (13)$$

$$\alpha_f = \frac{2\sin\psi}{\sqrt{3}(3 + y\sin\phi_1)} \quad (14)$$

$$\psi = \begin{cases} \phi_0 + (\psi_f - \phi_0)\sqrt{2\omega - \omega^2} & \omega \le 1 \\ \psi_f & \omega > 1 \end{cases} \quad (15)$$

with a defined mobilized dilatancy angle ψ. For $\phi = \psi$, we have $f = g$ and the classic associated flow rule is recovered while for $\phi \neq \psi$ non-associated flow rule is conducted. Values of ϕ_1 and ϕ_0 are fixed where $\phi_1 = 14^0$ and $\phi = 5^0$ were suggested[6]. Based on experimental observation, a number of constitutive equations for reinforced concrete in tension are suggested by means of tension stiffening phenomenon. This phenomenon is mainly affected by reinforcement ratio[16]. In the present constitutive model, the notation η in Eqs.5 and 6 is tension stiffening, which has a softening nature is expressed as

$$\eta = \eta_0 \exp(-\frac{\omega}{b_s}) \quad (16)$$

in which b_s is a function of steel ratio (Eq.19) and η_0 is the tensile strength on hydrostatic axis which is also close to the uniaxial tensile strength. The damage parameter ω defines the damage of material accumulated due to progressive growth of the micro cracks and can be defined in the form of

$$\omega = \frac{\beta}{\sigma_e \varepsilon_0} \int dW^p$$

(17) where σ_e is the effective stress, W^p denotes the plastic work accumulated after the initial failure which is

$$dW^p = \sigma_{ij}\, d\varepsilon_{ij} \quad (18)$$

β is a material constant and ε_0 is a constant value which is fixed at $\varepsilon_0 = 0.002$ or is an experimental data (for more details see 6)). Parameter β is an important material constant in defining damage parameter which has effect on compressive strain as well as softening branch of tension behavior rather than compressive and tensile strength of concrete. By comparing with the Kupfer's experimental results[12] $\beta = 0.4$ is proposed[6]. Although the experiment of Kupfer was conducted for plain concrete but due to investigation of Tanabe *et al.*[6], $\beta = 0.4$ yields acceptable results in reinforced concrete constitutive model as well.

The notation b_s also can be defined based on reinforcement ratio as

$$b_s = \begin{cases} 0.209\exp(-1.228\rho) + 0.07 & \rho \ge \rho_{\min} \\ 0.06 & \rho < \rho_{\min} \end{cases} \quad (19)$$

where $\rho = \rho_x \cos^2\theta_{cr} + \rho_y \sin^2\theta_{cr}$ and $\rho_{\min} = 0.4\%$. Parameters ρ_x, ρ_y are reinforcement ratios for the x and y direction respectively and θ_{cr} denotes the angle of initially formed crack to x-axis.

By using basic concept of classical theory of hardening plasticity[13], tangential constitutive matrix based on the isotropic hardening rule which is correspond to $\mathbf{D}_c$ matrix (Eq.1) can be written as

$$D_{ijkl} = D^e_{ijkl} - \frac{D^e_{ijtu}\dfrac{\partial f}{\partial \sigma_{rs}}\dfrac{\partial g}{\partial \sigma_{tu}} D^e_{rslk}}{\dfrac{\partial f}{\partial \sigma_{mn}} D^e_{mnpq} \dfrac{\partial g}{\partial \sigma_{pq}} + h} \quad (20)$$

with definition of hardening or softening function for hardening and softening material consequently as

$$h = -\frac{\partial f}{\partial W^p}\sigma_{ij}\frac{\partial g}{\partial \sigma_{ij}} \quad (21)$$

then stress is defined by using D_{ijkl} as follow

$$\dot{\sigma}_{ij} = D_{ijkl}\,\dot{\varepsilon}_{kl} \quad (22)$$

Application of the above formulations has been examined for numerical analysis at section 4.

3. MECHANISM OF LOCALIZATION AND POST-PEAK BEHAVIOR

Localization is a phenomenon that large strain accumulates inside a part of material without substantially affecting the strain in the surrounding materials (**Figs.2** and **4**). Once this phenomenon

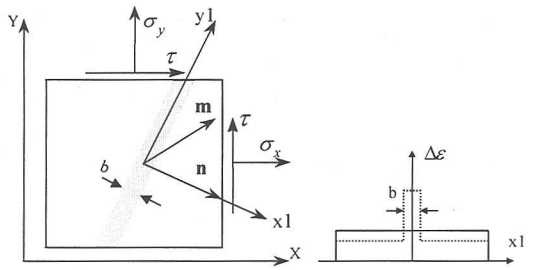

Fig.2 Localized damage band and strain jump

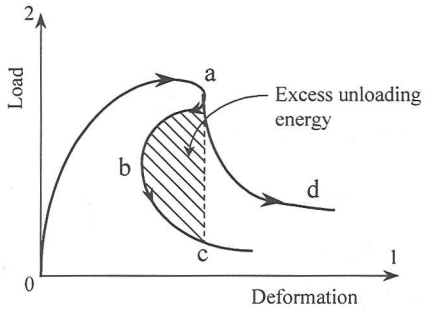

Fig.3 Load-deformation behavior of structure

occurs near to the peak point of loading, the behavior of structure is changed after this point and shear band will be formed regarding to strain accumulation within this part of structure. Shear band formation is clearly seen in the experimental observations of Vecchio and Collins[11] (**Fig.4**).

(1) Initiation of localization and shear band formation

As it is known that material instability which can be possibly led to the localization phenomenon in structures, occurs when acoustic tensor losses its positive definiteness. The physical mechanism for this phenomenon is that strain field across the damage band can possibly take a jump, while the equilibrium of the stress across the damage band remains to be satisfied (**Fig.2**).

The crack is regarded as a jump in displacements (Ortiz *et al.*[10],1987) or the displacement gradients (Belytschko *et al.*[5], 1988). This jump function can be added to the standard shape functions of the finite element. Moreover, discontinuous bifurcation can be formulated in constitutive equation level of material or composite material based on above-mentioned theory. To derive under what condition this kind of localization is triggered, we will adopt the element level bifurcation analysis of Ortiz, *et al.*[10] and use it in constitutive equation level analysis rather than finite element. The criteria for this kind of localization phenomenon can be expressed as

$$det\,(\mathbf{A}(\mathbf{n}))=0 \qquad (23)$$

where $\mathbf{A}(\mathbf{n})$ is the acoustic tensor for composite material. Eq.23 can be rewritten as:

$$A_{ij}(n)m_k = (n_i D_{ijkl} n_l)m_k = 0 \qquad (24)$$

where D_{ijkl} is the tangential constitutive matrix of the material. If the material satisfies Eq.24, then increments of strain can have a jump along the discontinuous surface (**Fig.2**). In fact crack direction is changed at final stages in many cases while localization occurs. This newly formed crack which is usually wider than previous cracks is called shear band. In other words, crack occurs when yield function is satisfied but shear band initiates once acoustic tensor looses its positive definiteness. The direction of crack is not necessarily constant and can rotate during analysis but the direction of shear band is kept constant for all steps after localization in this study and it is different from multi crack direction model.

Vector $\mathbf{n}$ is perpendicular to the discontinuity surface while vector $\mathbf{m}$ defines sliding direction. Based on this definition, $\mathbf{n}^T\mathbf{m}$ can define the type of failure. For a pure *Mode-I*, $\mathbf{m}$ is aligned with $\mathbf{n}$ and $\mathbf{n}^T\mathbf{m}=1$, on the other hand for a pure *Mode-II*, $\mathbf{m}$ is perpendicular to $\mathbf{n}$ then $\mathbf{n}^T\mathbf{m}=0$. Alternatively the first condition is related to the tension failure and the second one indicates shear failure. Likewise between two amounts is possible, which shows mixed mode of failure in the element.

(2) Post-peak behavior after localization

After the localization of the deformation in a structure, if we continue loading then loading continue in the localized part due to strain accumulation in shear band while the other parts are elastically unloading. It is notable that in two parts, stress is in equilibrium across discontinuous plane but strain is different in localized and non-localized zone so each part shows different behavior particularly.

In this process, the unloading region of structure releases a quantity of strain energy given by

$$w_u = \int_{V_u} (\sigma . d\varepsilon)\mathrm{d}V \qquad (25)$$

and the energy supplied to the localized band is obtained by

$$w_l = \int_{V_l} (\sigma . d\varepsilon) \mathrm{d}V \qquad (26)$$

which V_u and V_l are volume of the unloading part and localized band respectively. Eqs.(25) and (26) are valid for admissible strains. When the magnitude of energy released is less than the energy supplied, i.e. in the structure, then it is stable state under displacement control loading. It means that load decreases while deformation is increased. This kind of behavior is shown in **Fig.3** (curve 'ad'). For this condition we have

$$|w_u| < |w_l| \qquad (27)$$

which shows stable state of structure. On the other hand when the magnitude of energy released is bigger than the energy supplied or

$$|w_u| > |w_l| \qquad (28)$$

the structure is in unstable state even under displacement control condition. This type of load-deformation behavior is called "snap-back"(curve 'abc' in **Fig.3**). The shaded area in the figure denotes the excess unloading energy. If the deformation at point 'a' is maintained constant, then the load drops suddenly from 'a' to 'c' without any significant overall deformation. The actual load-deformation path followed is 'abc' which is of the snap-back type. Excess unloading energy w_a can be written as

$$w_a = |w_u| - |w_l| \qquad (29)$$

To circumvent this problem in computational analysis, one may use the Arc-length method[7),8)] for finite element formulation. This method has been tried to overcome this problem in fracture types of analyses in Nagoya University successfully. But for the calculation on constitutive level, the authors have used a special form of load control analysis where stress increases incrementally upon to the peak. Once peak point is signaled based on Eq.23 or any suitable stability criterion, stress decreases while strain is obtained by using tangential stiffness tensor. This method has covered both pre-peak and post-peak behavior for either snap-through or snap-back instabilities and gives real load-deformation path 'abc' as shown in **Fig.3**.

Analyses have been carried out for both cases of associated and non-associated plasticity flow rule. For the case of non-associated flow rule, localization usually signals before peak point of loading by using Eq.23. This gives an artificial point for peak point and it means that loading should be decreased in spite of being in hardening branch of loading. In the other words, peak point and the point where localization occurs are not coinciding to each other in this case. To overcome this problem and get real peak point, first Drucker's stability postulate, which is also called stability of small [13)], is adopted here. By applying the principal of virtual work, the stability condition can be written as

$$\int_V \dot{\sigma}_{ij}\, \dot{\varepsilon}_{ij}\, dV > 0 \quad \text{or} \quad \dot{\sigma}_{ij}\, \dot{\varepsilon}_{ij} > 0 \qquad (30)$$

where V is an arbitrary volume. As long as above equation is positive, stability is assured. When Eq.30 passes zero point and become negative, structure will go to the post-peak or softening branch. The method can capture either snap-through or snap-back instability in constitutive equation level of analysis.

(3) Constitutive equation when localization has been initiated

In section 2, constitutive equation based on modified Drucker-Prager model has been represented in detail. The model can be used before localization initiation due to Eq.23. After that localization signals and Eq.23 is satisfied, a shear band can be formed then the strain field within the element will no longer be uniform. Once localization occurs, strain is increased inside shear band while in the outside regions, elastic unloading appears and strain will be decreased. This phenomenon can be seen clearly in **Fig.4**. To consider shear band in constitutive equation, complementary tensor C_{ijkl} is used instead of stiffness tensor D_{ijkl}. Matrices C_{ijkl}, C^e_{ijkl}, C^l_{ijkl}, (i, j, k=1,2,3) are the components of the complementary tensors for the element, the elastically unloading part of the element, and the localized band respectively. It is notable that before localization, strain field is uniform and can be calculated based on elastic, elasto-plastic stiffness or complementary tensors depend on constitutive equation but after localization, material outside shear band starts to be unloading elastically while inside shear band is loading as an elato-plastic type of material but not essentially the same as before.

In this study, the authors used initial elastic constitutive matrix for unloading part and different elasto-plastic tangential constitutive matrix for shear band due to different hardening (or softening) function of h in Eq.20. For instance, softening function for shear band is $4h$ for the presented analyses while h is softening function of material after the peak without shear band formation

Table 1 Material properties for specimens PV10, PV11, PV19, PV23 and PV25

Specimen	σ/τ	ρ_ℓ%	$f_{y\ell}$ (MPa)	ρ_t%	f_{yt}	ε_0	f'_c (MPa)	Failure Mode
PV10	-0.00/1.0	1.785	276	0.999	276	0.0027	14.5	II
PV11	-0.00/1.0	1.785	235	1.306	235	0.0026	15.6	I
PV19	-0.00/1.0	1.785	458	0.713	299	0.0022	19.0	II
PV23	-0.39/1.0	1.785	518	1.785	518	0.0020	20.5	II
PV25	-0.69/1.0	1.785	466	1.785	466	0.0018	19.2	II

(conventional method). The value of the softening function of shear band used here is just to examine the theory since there is no experimental data in this regard. The effective complementary tensor of the element can be calculated by assuming that the stress is homogeneous throughout the localized element. In other word, despite the strain field, stress is continuos all over the element as well as across discontinuity planes.

In the discontinuity element, a length scale parameter is introduced which is a material parameter and can be related to the size of the fracture process zone. Based on **Fig.2** and assuming that shear bandwidth and element equivalent sizes are b and L respectively, equivalent strain within an element is

$$d\varepsilon = (1-\frac{b}{L})d\varepsilon^u + \frac{b}{L}d\varepsilon^l \qquad (31)$$

where

$$d\varepsilon_{ij} = C_{ijkl}.d\sigma_{kl} \qquad (32)$$

$$d\varepsilon^u_{ij} = C^e_{ijkl}.d\sigma^e_{kl} \qquad (33)$$

$$d\varepsilon^l_{ij} = C^l_{ijkl}.d\sigma^l_{kl} \qquad (34)$$

and $L=\sqrt{A}$ where A is the element area therefore Eq.31 can be rewritten as

$$C_{ijkl}.d\sigma_{kl} = (1-\frac{b}{L})C^e_{ijkl}.d\sigma^u_{kl} + \frac{b}{L}C^l_{ijkl}.d\sigma^l_{kl} \qquad (35)$$

Equilibrium across discontinuity planes requires that stress be uniform then

$$d\sigma_{ij} = d\sigma^e_{ij} = d\sigma^l_{ij} \qquad (36)$$

where $d\sigma_{ij}$, $d\sigma^e_{ij}$ and $d\sigma^l_{ij}$ denote of equivalent stress increment within an element, stress increment in unloading part and stress increment in shear band respectively. Combining (35) and (36)

$$C_{ijkl} = (1-\frac{b}{L})C^e_{ijkl} + \frac{b}{L}C^l_{ijkl} \qquad (37)$$

Now, using the above assumption of stress homogeneity within the element (Eq.36) together with Eqs.32, 33 and 34, strain in unloading and localized part can be defined as

$$d\varepsilon^u_{ij} = C^e_{ijpq}(C_{pqrs})^{-1}d\varepsilon_{rs} \qquad (38)$$

and

$$d\varepsilon^l_{ij} = C^l_{ijpq}(C_{pqrs})^{-1}d\varepsilon_{rs} \qquad (39)$$

(the superscript '-1' denotes matrix inversion). For the case $b=L$, although Eq.23 is satisfied but in fact no shear band is formed or in the other words, all parts of element are loading due to loading process. Hence we can set $C_{ijkl} = C^l_{ijkl}$ where C_{ijkl} can be calculated by section 2, which is equal to $[D_{ijkl}]^{-1}$.

4. NUMERICAL INVESTIGATION IN CONSTITUTIVE EQUATION LEVEL

In order to evaluate the capability of the described model as well as to see post-peak behavior based on mentioned formulations, five reinforced concrete panels tested by Vecchio and Collins are analyzed and checked to see whether aforementioned kind of localization is detected or not. In those experiments, the panels were loaded monotonically and cyclically through five shear keys around the perimeter on each specimen. The dimensions of all square panels are the same and kept constant as 89cm × 89cm × 7cm subjected to plane stress load condition. The loading possibilities were not restricted to pure shear and any combination of shear and tension as well as compression could be produced by varying the magnitude and direction of the forces in the links. In this experiment, 26 specimens were tested under various combinations of the external forces as reported in reference 11).

Based on experimental observation, it is obvious that this kind of localization can just be detected in

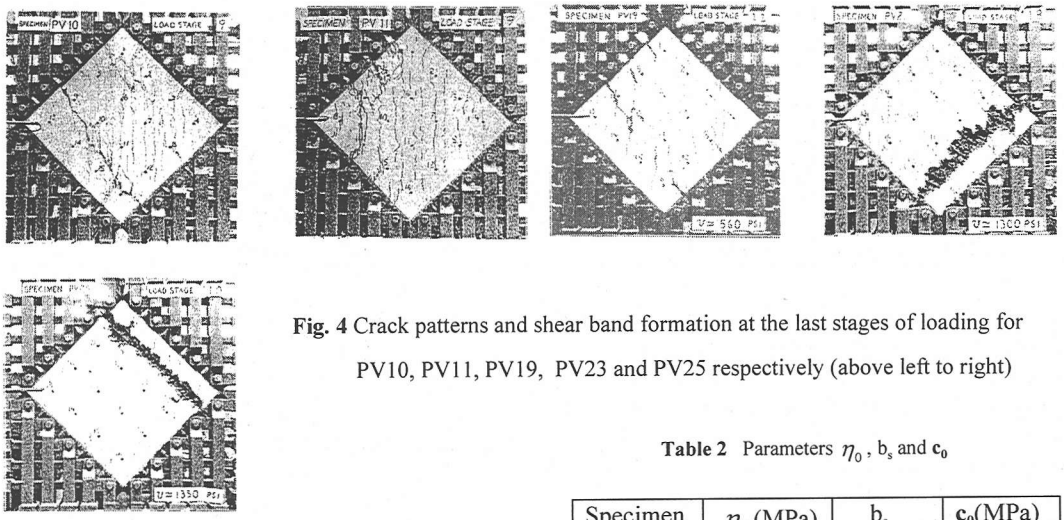

Fig. 4 Crack patterns and shear band formation at the last stages of loading for PV10, PV11, PV19, PV23 and PV25 respectively (above left to right)

RC panels, which failed in shear in *Mode-II*. In *Mode-I*, either the longitudinal or transverse reinforcements yielded and directions of the final cracks are almost the same as initially formed cracks. For this mode, cracks direction can be easily calculated by principal stresses directions while in *Mode-II*, the final cracks directions are considerably different than initially formed cracks so can not be found by the conventional method such as principal stresses directions. In other words, for most cases of failure in *Mode-II*, in fact at the final load stages near to the peak point, before or after that, a shear band will form due to loss of shear capacity of concrete as well as aggregate interlock which is independent to initially formed cracks as have been observed by experiments.

For *Mode-II*, two failure types can be taken into consideration as they were observed in experiments as follows:

1. Sliding shear failure of the concrete after yielding of the transverse steel but prior to yielding of the longitudinal steel; or
2. Sliding shear failure of concrete prior to yielding of either the longitudinal or transverse steel.

Panels PV11 is analyzed here for *Mode-I* along with PV10, PV19, PV23 and PV25 for failure *Mode-II*. In panels PV23 and PV25 forming of shear band has been reported and observed by failure patterns.

All panels are analyzed using both associated and non-associated flow rule. As will be shown in the results, although associated flow rule gives reasonable results but non-associated flow rule yields much closer prediction to experiment. This fact has been mentioned by other researcher as well. Major parameters used in the method are given in **Table 2**.

Table 2 Parameters η_0, b_s and c_0

Specimen	η_0 (MPa)	b_s	c_0(MPa)
PV10	2.89	0.11	10.60
PV11	2.31	0.10	11.38
PV19	3.33	0.12	15.84
PV23	3.28	0.09	15.00
PV25	2.69	0.09	14.35

(1) Analysis of panel PV10

This panel failed in *Mode-II* and shear failure of concrete prior to yielding of longitudinal steel has been reported. Material properties are given in Table 1 and specimen was under monotonic pure shear. **Fig.5** shows the response of shear stress in terms of shear strain for both non-associated and associated flow rule along with experimental result. Agreement with experiment is better in the case of non-associated flow rule. Although the failure is in *Mode-II*, shear band does not form so no localization has signaled. Since shear band is never formed for this specimen, the directions of cracks can be found through principal stresses directions and they are 45° based on loading condition. Cracks directions reported by experiment are 45° but in the last stages of loading, after yielding of transverse reinforcement, cracks shifted direction to become more acute to longitudinal direction.

(2) Analysis of panel PV11

This panel failed in *Mode-I* and yielding of both longitudinal and transverse steel has been reported. Material properties are given in **Table 1** and specimen was under monotonic pure shear. **Fig.6** shows the response of shear stress in terms of shear strain for both non-associated and associated plasticity along with experimental result.

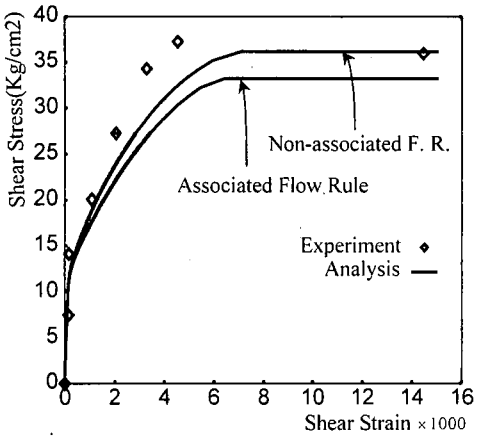

Fig.5 Shear stress versus shear strain for PV10

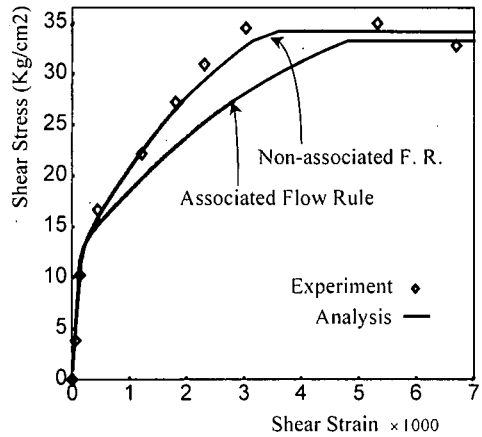

Fig.6 Shear stress versus shear strain for PV11

Agreement with experiment is good in the case of using associated flow rule but much closer to experiment for non-associated flow rule. Since the failure is in *Mode-I*, no localization has signaled so the direction of cracks will be 45° based on loading condition. Observed crack direction is also 45° until last stage of loading (**Fig.4**).

(3) Analysis of panel PV19

Shear failure occurs in this panel prior to yielding of longitudinal steel as has been reported by experiment. Although this panel fails in shear but shear band does not form as can be seen in failure pattern in **Fig.4**. This also has been found in analytical result and in fact, Eq.23 never satisfied for this panel and just yielding of steel was announced by program. Therefore crack directions are found through principal stress directions and they are 45° for this panel. Analytical results along with experimental result are shown in **Fig.7**. This figure shows the response of shear stress in terms of shear strain for both non-associated and associated flow rule comparing with experimental results. Both results have very good agreement with experiment. Material properties are given in Table 1 and specimen was under monotonic pure shear.

(4) Analysis of panels PV23 and PV25

To examine capability of the model in analyzing shear failure when shear band is formed, panels' PV23 and PV25 are analyzed here. These two panels failed in shear (*Mode-II*) prior to yielding of steel as reported by experiment and also obtained by analysis. **Figs.8** and **9** show the response of shear stress in terms of shear strain for both non-associated and associated flow rule along with experimental results. For both specimens, shear bands formed in different directions than initially formed cracks and parallel to one of the element edges, which can be seen in **Fig.4**.

In localization analysis of these specimens, shear band formation has signaled and direction of shear band '**n**' is calculated by analysis and compared with experimental observation (**Fig.4**). Sliding direction '**m**', which is also obtained by Eq.24 is given together with vector **n** and experimental observation of shear band direction in **Table 3**. This comparison shows that the results are reliable enough to predict reinforced concrete response in shear failure process.

Figs.8 and **9** show that analytical results are in good agreement with experiment in two cases of associated and non-associated plasticity for both specimens but much closer for latter one. In the points denoted by Δ, localization occurs and $det\mathbf{A}(\mathbf{n})=0$ so vectors **m** and **n** find amounts as given in Table 3. After this point, shear band forms in the specimens and regarding to shear bandwidth, we will be able to predict post-peak behavior of specimens based on presented formulations in previous section (Eqs.31-39). Shear bandwidth for both PV23 and PV25 measured from experimental observation is 10cm approximately. Applying mentioned bandwidth to Eq.37, constitutive matrix for post-peak regime was predicted. Pre-peak and post-peak predictions of both specimens PV23 and PV25 are shown in **Figs.10** and **11** respectively. It is obvious that shear band direction given in **Table 3** should be compared with shear band formed at the last stages of loading in experiment procedure not initially formed crack patterns (**Fig.4**, PV23 and PV25).

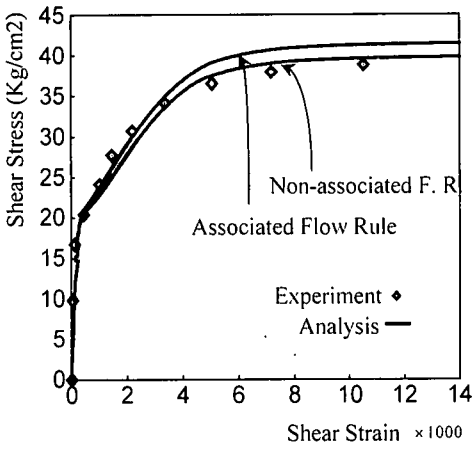

Fig.7 Shear stress versus shear strain for PV19

The authors could not found any post-peak experimental response of RC elements therefore such analyses should be calibrated by further experiments. Results however seem to be reasonable for post-peak behavior of elements failed in shear. Before peak point of loading, the stress-strain relationship is followed by elasto-plastic constitutive equation while after that however drastic drop of strength occurs due to shear band formation in the specimen.

The difference between two analyses is that in the first one (**Figs. 8** and **9**), shear bandwidth is not taken into analyses as a thin band embedded in element and in fact, shear bandwidth is equal to the length of element L. In other words as mentioned before, all parts of the element are loading without localized band formation and also without unloading portion. However, shear band as a thin layer is included in constitutive equation embedded within the element and shear bandwidth is taken approximately equal to those observed in experiment. As for descending branch after localization, it is a function of both stiffness matrix of the linearly unloading zone and elasto-plastic matrix of loading region outside and inside shear band respectively. Therefore in the specimen with thin shear band or in other words, specimen with big unloading part, post-peak behavior is dominated by elastically unloading part than loading part so the path is closer to linear form than curvature particularly in **Fig.11**.

In specimen PV25, snap-back occurs after peak point of loading (**Fig.11**). It is predicted that if we set such an experimental apparatus to go beyond peak, this kind of instability (snap-back) might be observed in some kind of shear failure of RC elements where shear band is comparatively thin. It

Table 3 Shear band and sliding directions

Specimen	θ_m	θ_n Analysis	θ_n Exp.
PV23	83.0	8.5	0
PV25	75.0	13.6	0

is clear that shear bandwidth has a key role in our post-peak study and for instance, if we set larger bandwidth, snap-back instability may not occur in analysis procedure.

5. CONCLUSION

In this paper, pre-peak as well as post-peak behavior of reinforced concrete panels have been analyzed. Pre-peak behavior based on modified Drucker-Prager model is analyzed while post-peak regime is captured by using constitutive equation of localized element with a shear band region based on complementary matrix. In the modified Drucker-Prager method three major nonlinear factors for concrete in reinforced concrete structures are considered as follows:

1. Tension stiffening effect
2. Compression strength reduction due to transverse tensile strain
3. Shear transfer at the crack surface

so the method can be used as a unified plastic model for concrete. The analyses of five panels tested by Vecchio *et al.*[11] have been conducted for non-associated and associated flow rule analysis while determinant of acoustic tensor ($det.\mathbf{A}(\mathbf{n})$) signals localization. As seen before, determinant of acoustic tensor passes zero point just in some cases of failure in *Mode-II* or shear failure. In those cases, shear band direction can be found with solving $det.\mathbf{A}(\mathbf{n})=0$ for $\mathbf{n}$ vector while $\mathbf{n}$ is normal to shear band direction. For all analyzed panels, although associated flow rule gives reasonable results but the results of non-associated flow rule were much closer to the experiments.

Post-peak behavior of structures also has been analyzed by using a special form of constitutive equation including shear band effects based on complementary matrix. Peak point of loading is signaled by means of singularity of acoustic or localization tensor. After this point is reached, a shear band is formed and element goes to post-peak branch of loading which can be led to a special form of instability so-called snap-back behavior. Snap-back instability occurred analytically in the specimen PV25. The results of post-peak regime seem to be reasonable but need to be evaluated by further experiments.

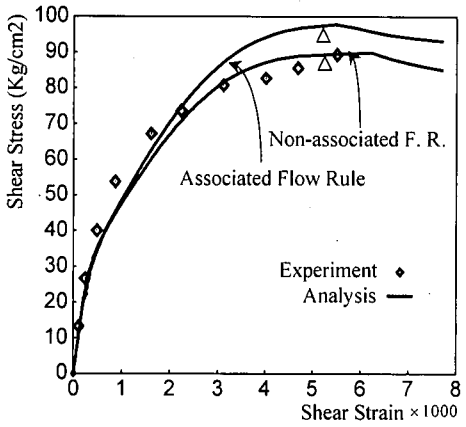

Fig.9 Shear stress versus shear strain for PV25

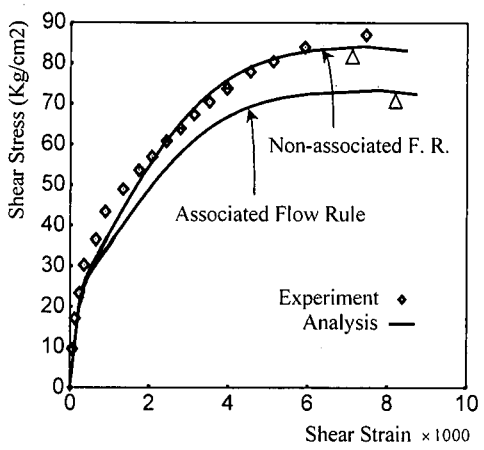

Fig. 8 Shear stress versus shear strain for PV23

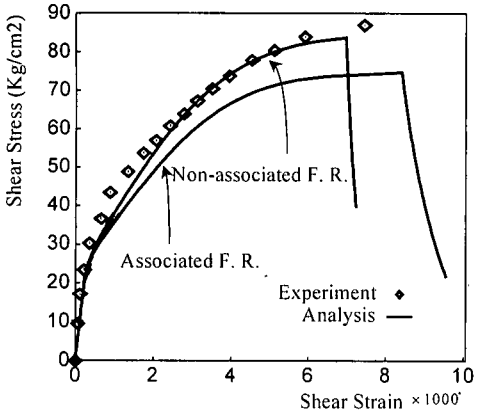

Fig.10 Shear stress versus shear strain for PV23

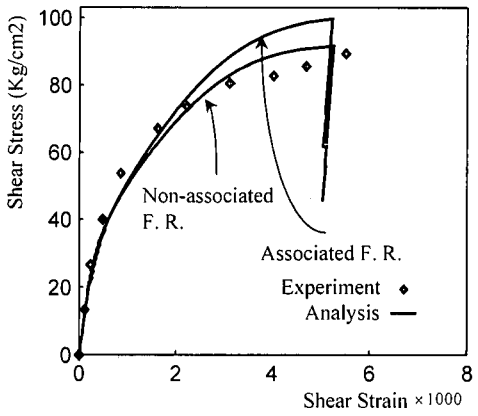

Fig. 11 Shear stress versus shear strain for PV25

REFERENCES

1) Bazant, Z. P. and Lin, F. B.: Stability against localization of softening into ellipsoids and bands; Parameter study, Int. J. Solids Structures, Vol. 25, No. 12, pp. 1483-1498, 1989.
2) Singh, U. K. and Digby, P. J.: A continuum damage model for simulation of the progressive failure of brittle rocks, Int. J. Solids Structures, Vol. 25, pp. 647-663, 1989.
3) Belytschko, T., Fish, J. and Engelmann, E.: A finite element with embedded localization zones, J. Comput. Meths. In Appl. and Mech. Engrg. ,70, pp. 59-89, 1988.
4) Tanabe, T., Yu, G. and Salamy, M.R.: Analysis of the localized failure phenomenon in reinforced concrete shear walls,Conference on comp. modeling of concrete structures, Badgastein, Austria, pp. 265-274, 31 March-3 April 1998.
5) Salamy, M.R., Yu, G. and Tanabe, T.: Analysis of shear failure in RC beams considering localization phenomenon, JSCE, No.648, V-47, pp. 253-264, May 2000.
6) Tanabe, T., Wu, Z. and Yu, G.: A unified plastic model for concrete, JSCE, No.496, V-24, pp. 21-29, Aug. 1994
7) Crisfield, M. A.: An Arc-length method including line searches and acceleration, Int. J. Num. Meth. Engrg., Vol.19, pp. 1269-1289, 1983.
8) Crisfield, M. A.: Non-linear finite element analysis of solids and structures, John Wiley & sons, Vol.1, pp. 266-286, 1991.
9) Hill, R.: Acceleration waves in solids, J. Mech. Phys. Solids, Vol. 10, pp. 1-16, 1962.
10) Ortiz, M. , Leory, Y. and Needlemann, A.: A finite element method for localized failure analysis, J. Comput. Meths. In Appl. and Mech. Engrg., 61, pp.189-214, 1987.
11) Vecchio, F. and Collins, M. P.: The response of reinforced concrete to In-plane shear and normal stresses, University of Toronto Publication, No.82-03, March 1982.
12) Kupfer, H., Hilsdorf, H. K. and Rusch, H.: Behavior of concrete under biaxial stresses, ACI Journal, Vol.66, No.8, pp. 656-636, Aug. 1969.
13) Chen, W. F.: Plasticity in reinforced concrete, 1992.

14) Yu, G.: Study of Localization phenomenon in reinforced concrete structures, Doctoral dissertation, Civil Eng. Dept. of Nagoya University, March, 1995.
15) US-Japan joint Seminar on post-peak behavior of RC structures subjected to seismic loads, Yamanashi, Japan, October 1999.
16) Okamura, H and Maekawa, K.: Nonlinear analysis and constitutive models of reinforced concrete, pp.28-60, 1991.

(Received April 3, 2000)

統一塑性モデルを用いたRC板及びポストピーク挙動の解析

Mohammad Reza SALAMY・田辺　忠顕

本研究では，異なる応力場におけるコンクリートの挙動を一つの基準で記述するために考えられた，統一化塑性モデルを用いた．このモデルは，ひび割れやtension stiffening，せん断伝達や圧縮強度の低下といったコンクリートの主な非線形現象を取り扱うことが可能である．RC要素が最大耐荷力付近の分岐点を通過する際の破壊モードやshear bandの方向を定義するために，局所指標が用いられる．局所化現象は，材料のacoustic tensor $\mathbf{A(n)}$ が正値でなくなる時に生じる（もしくは．$det\ \mathbf{A(n)} = 0$）．本研究では，この手法をVecchioやCollinsらの実験結果と比較することにより評価した．